

Simulation of surface segregation free energies

J. D. Rittner

*Department of Materials Science and Engineering and the Materials Research Center, Northwestern University,
Evanston, Illinois 60208-3108*

S. M. Foiles

Sandia National Laboratories, Computational Materials Science Department, Livermore, California 94551-0949

D. N. Seidman

*Department of Materials Science and Engineering and the Materials Research Center, Northwestern University,
Evanston, Illinois 60208-3108*

(Received 7 April 1994; revised manuscript received 25 July 1994)

The effects of different assumptions made in the simulation of surface segregation free energies are considered. Thirty face-centered-cubic dilute binary alloys are investigated using embedded-atom method potentials. First, it is demonstrated that the inclusion of local atomic relaxations in lattice statics simulations strongly affects the segregation free energy at (111) free surfaces in over half of the alloys. Second, a Monte Carlo technique, namely, the overlapping distributions method (ODMC), is used to determine the effect of the vibrational entropy term on the surface segregation Helmholtz free energy for simulations at elevated temperatures (1000 K). It is determined that the vibrational entropy term is important for a quarter of the alloys. We conclude that for accurate calculations of surface segregation free energies, both local atomic relaxations and the vibrational entropy must be included in nearly all cases. Since the ODMC method is very computer-time intensive, a technique based on a simplification of the quasiharmonic approximation for calculating free energies is investigated. Results from this free-energy minimization (FEM) method using the local harmonic approximation are compared to results from the ODMC method. It is found that the FEM method calculates the segregation free energies at (111) free surfaces accurately for most of the 30 alloys. Segregation free energy profiles are also calculated as a function of distance from (111) free surfaces employing both methodologies. The agreement is found to be poor for alloys that have a large solvent atom and a small solute atom. Other problems and sources of error with the FEM method are also discussed.

I. INTRODUCTION

The subject of segregation of solute atoms to free surfaces has received a great deal of experimental and theoretical attention, because of both basic and practical interest in this phenomenon.¹⁻⁴ The theoretical efforts have been directed toward determining the thermal equilibrium structures and compositions of alloys at free surfaces.⁵⁻⁸ The simplest model assumes that the atoms sit rigidly on their perfect lattices sites.^{9,10} A more realistic approach allows the atoms to relax from their ideal lattice sites to the minimum-energy configuration. Another effect related to atomic relaxations is the entropy due to vibrations of the atoms. Atoms in the vicinity of a crystal defect, such as free surface, generally have different vibrational frequencies than they do in the bulk; this gives rise to a vibrational entropy contribution¹¹ that may also play a role in determining the thermal equilibrium structures and compositions of alloys in the vicinity of free surfaces, especially at elevated temperatures. With each additional physical effect considered, the computer simulation methodologies that must be employed become more complicated and computer-resource intensive. The usual way to include local atomic relaxations is to employ a lattice-statics simulation. The vibrational entropy can

be included by employing simulation techniques such as the Monte Carlo (MC) or molecular dynamics (MD) methodologies. Thus, the first topic we investigate in this paper is the relative importance of atomic relaxations and vibrational entropy on solute-atom segregation to a (111) free surface for 30 solvent-solute atom pairs constructed from six different face-centered-cubic elements—Ag, Au, Cu, Ni, Pd, and Pt—employing embedded-atom method (EAM) potentials.¹²

In addition to being resource intensive, another drawback to MD and MC simulations is the difficulty of obtaining quantities such as the entropy or free energy directly. Recently, a new deterministic approach has been introduced by Srolovitz *et al.*: the free-energy-minimization (FEM) method.^{13,14} This method has been promoted as an alternative to MC or MD simulations. The FEM method calculates the free energy of an ensemble directly by including approximations of the configurational and vibrational entropy terms. Local atomic relaxations are calculated by minimizing the free energy with respect to the atomic coordinates. Solute-atom segregation can also be studied by minimizing the free energy with respect to the composition at each atomic site. The power of this methodology is that the computer time it requires has been reported to be of the same

order of magnitude as lattice statics simulations. The computational efficiency of this methodology is the result of making several important approximations in calculating the free energy. A very similar methodology, the second moment (SM) approximation, has also been proposed recently by Sutton.¹⁵ The SM approximation is not investigated in this paper as it is expected to produce results similar to the FEM method.

Because of its computational efficiency, the FEM method is becoming widely used.^{13,14,16,17} Because it is an approximate technique, it is important to know the effects that the approximations can have on the results produced. Only a few comparisons have been made between FEM method results and experimental data or the results from more accurate simulation techniques. Two papers compared bulk crystal properties of Cu (Ref. 13) and Au (Ref. 17) computed with the FEM method to results from more accurate MC simulations. Another paper¹⁴ compared segregation profiles of CuNi alloys for several free surfaces and twist grain boundaries computed with both the MC and FEM methods. Recently,¹⁸ a study of the accuracy of the FEM method in the calculation of bulk and defect properties of Cu as a function of temperature has been reported. From these few comparisons it appears that this methodology is best suited to calculating bulk properties. It also does a reasonably good job of calculating segregation profiles to free surfaces and grain boundaries in the CuNi alloy system, especially on the copper-rich side of the phase diagram. It is not clear, however, that this is necessarily true for other alloys. That is, CuNi may not be a representative test case; the CuNi phase diagram exhibits complete solid solubility at the temperatures studied. This is important since it has been widely observed experimentally^{3,19} that the level of segregation is inversely proportional to the maximum solid solubility of the alloy. Another important parameter in determining the level of segregation is the size misfit between the solute and solvent atoms.^{5,20} The difference in the lattice constants between nickel and copper is only 2.6%.

Thus, the second topic we examine in this paper is the effect of using different alloys on the accuracy of the FEM method in simulating surface segregation free energies. We determine the accuracy of the FEM method by comparing Helmholtz binding free energies calculated with the FEM method to those calculated with a MC technique—the overlapping distributions Monte Carlo (ODMC) method. Helmholtz binding free energies of a solute atom to the outermost plane of a (111) free surface are computed for the 30 solvent-solute alloy combinations. Another comparison examines the Helmholtz binding free energy profiles for segregation to (111) free surfaces for three dilute alloys—Pt(Au), Ni(Cu), and Ni(Pd).

In Sec. II we present a general overview of the computational procedures utilized to perform the simulations. We also give a brief explanation of the different methodologies employed to calculate the Helmholtz free energies—the FEM and the overlapping-distributions Monte Carlo method. In Sec. III we present the results from the simulations and discuss the effect of local atom-

ic relaxations and vibrational entropy on surface segregation free energies. We also discuss the results of the comparisons between the FEM and the ODMC methods. Finally, in Sec. IV we list the general conclusions of this study.

II. COMPUTATIONAL PROCEDURE AND METHODOLOGIES

The three methodologies used in this study—lattice statics, ODMC, and FEM—all employed embedded-atom method potentials. To determine the atomic structure of free surfaces, a relatively simple model of the energies is required so that a sufficiently large set of atoms can be considered. The EAM potentials are a good choice for such studies since previous work has shown that they provide a reasonable description of the energetics of metallic systems, yet they do not require significantly more computational effort than the use of simple pairwise interaction models.²¹ In the EAM model, much of the binding energy of the solid is attributed to the energy associated with embedding each atom into the local electron density provided by the remaining atoms of the system. This energy is assumed to depend only on the type of atom being embedded and the local electron density. Thus, the same embedding energy applies in pure metals as in an alloy. This embedding contribution is supplemented by a pairwise interaction term that accounts for core-core interactions. The embedding energies and pairwise interactions required by the model are determined empirically by fitting them to various experimental data.

Instead of examining compositions to measure solute-atom segregation, we use a more fundamental quantity, the Helmholtz binding free energy of a substitutional solute atom to different atomic sites in the vicinity of a free surface. At the dilute limit of one component in another or if there are no solute-atom interactions, the Helmholtz binding free energy is a direct measure of solute-atom segregation. The Helmholtz binding free energy is also commonly called the segregation free energy since it is the energy that drives the segregation process. The segregation free energy $F_B(x)$ is defined by

$$F_B(x) \equiv \Delta F(\text{bulk crystal}) - \Delta F(x), \quad (1)$$

where $\Delta F(\text{bulk crystal})$ is the change in the Helmholtz free energy of an ensemble when a substitutional solute atom is dissolved in a bulk-crystal region far from any crystalline defects, and $\Delta F(x)$ is the change in the Helmholtz free energy when a substitutional solute atom is dissolved at a substitutional site x in the vicinity of a free surface. The quantity $F_B(x)$ is, therefore, the change in the Helmholtz free energy when a substitutional solute atom moves from a bulk-crystal region to a region near a free surface. The definition in Eq. (1) is such that a positive value of $F_B(x)$ implies an attractive interaction, while a negative value implies a repulsive interaction.

All of the simulations were performed using the same simulation conditions. The FEM and ODMC simulations were done at a temperature of 1000 K. The composition of each alloy was fixed at the dilute limit of one

component in the other. In practice, this means that there was only one solute atom at a time in each simulation cell. Periodic boundary conditions were used on the simulation cells to eliminate surface effects. The size of the simulation cells was large enough (6000 to 7000 atoms) to minimize finite-size effects. Figure 1 exhibits the dimensions of the simulation cells used in the simulation of surface segregation free energies. The simulation cell contains a crystal slab with (111) free surfaces and a nearly infinite region of vacuum on both sides of the slab in the x direction. The periodic boundaries make the slab infinite in the y and z directions. The periodic boundaries in the y and z directions were fixed at the lengths determined by the equilibrium value of the lattice constant for a perfect crystal at the simulation temperature. This was done to counteract the effect of surface tension. In nature, the volume of the bulk-crystal regions compared to the surface area is more than large enough to counteract the surface tension. In a finite-sized simulation cell, however, the surface tension may not be fully counteracted by the relatively small bulk-crystal region. Fixing the periodic boundaries in the directions perpendicular to the surface normal mimics an infinitely large bulk-crystal region. The periodic boundaries in the x direction were placed at very large distances from the crystalline slab to create regions of vacuum above the free surfaces. This also allowed the atomic planes to move in the direction normal to the surfaces, so that the simulations were performed at a constant pressure of 0 atm.

A. Lattice-statics method

The first effect on segregation free energies that we investigate is the effect of including local atomic relaxations. In the simplest approach to calculating segregation free energies—no local atomic relaxations—the total energy of the system is calculated with the atoms sitting at their ideal lattice positions right up to the surface. To include local atomic relaxations, a standard lattice statics routine is used. The atomic positions are adjusted using the conjugate gradient method until the total energy of the system is minimized. Since the entropy is being ignored for now, the segregation free energies can be

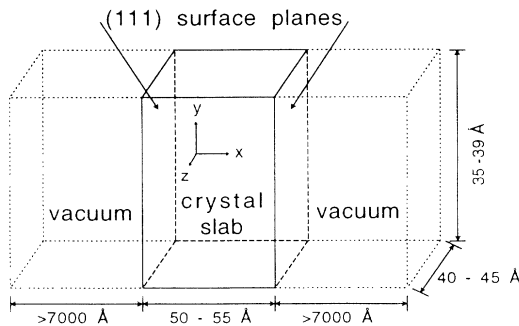


FIG. 1. Dimensions of the simulation cells. The simulation cell contains a crystal slab with (111) free surfaces and a nearly infinite region of vacuum on both sides of the slab in the x direction. The periodic boundaries make the slab infinite in the y and z directions.

found by using total internal energies in Eq. (1) instead of Helmholtz free energies. For $\Delta F(\text{bulk crystal})$ the total internal energy is calculated for a bulk crystal (no defects) both with and without a solute atom present. For $\Delta F(x)$, the total internal energy is calculated for a surface simulation cell both with and without a solute atom in the outermost surface plane.

B. Overlapping-distributions Monte Carlo method

The second effect on segregation free energies that we investigate is the effect of including the vibrational entropy. The Helmholtz free energy includes the vibrational entropy as well as the internal energy. The Helmholtz free energy cannot be expressed as an ensemble average. Hence, it is not possible to calculate it directly from a MC simulation. There are techniques available, however, that allow the use of MC simulations to calculate the Helmholtz free energy difference between two ensembles. These techniques include thermodynamic integration, Widom's particle insertion method,²² energy density functions,²³ and the overlapping distributions method.²⁴

The overlapping-distributions Monte Carlo method is derived as follows: From statistical mechanics, the Helmholtz free energy is given by

$$F = -kT \ln(Z), \quad (2)$$

where Z is the classical partition function that is given by

$$Z = \int e^{-H/kT} d\mathbf{p} d\mathbf{q}. \quad (3)$$

H is the Hamiltonian, \mathbf{p} and \mathbf{q} are the momentum and position vectors for the N atoms in the ensemble, and kT has its usual significance. The Hamiltonian is defined as

$$H = \sum_{i=1}^N \frac{\mathbf{p}_i^2}{2m_i} + E, \quad (4)$$

where E is the internal energy and m_i are the masses of the atoms. If all the atoms in an ensemble are the same type, then the partition function can be expressed as

$$Z = \left[\int e^{-\mathbf{p}^2/2mkT} d\mathbf{p} \right]^N \int e^{-E/kT} d\mathbf{q} = (2\pi mkT)^{3/2} Q, \quad (5)$$

where Q is the integral of $\exp(-E/kT)$ over all configuration space.

The change in the Helmholtz free energy on going from some arbitrary ensemble 1 to another arbitrary ensemble 2 is

$$\Delta F = F_2 - F_1 = -kT \ln \left(\frac{Z_2}{Z_1} \right), \quad (6)$$

where Z_1 and Z_2 are the partition functions of the respective ensembles. There is no restriction on what the difference is between ensemble 1 and ensemble 2. In this study ensemble 2 is found by replacing a specific atom in ensemble 1 with a solute atom, while leaving everything else the same. For these two ensembles, the ratio Z_2/Z_1

is then

$$\frac{Z_2}{Z_1} = \left(\frac{m_2}{m_1} \right)^{3/2} \frac{Q_2}{Q_1}. \quad (7)$$

Now using the definition of Q we find

$$\frac{Q_2}{Q_1} = \frac{\int e^{-E_2/kT} d\mathbf{q}}{\int e^{-E_1/kT} d\mathbf{q}} = \frac{\int e^{-(E_2-E_1)/kT} e^{-E_1/kT} d\mathbf{q}}{\int e^{-E_1/kT} d\mathbf{q}}. \quad (8)$$

This is in the form of a thermodynamic average over ensemble 1:

$$\frac{Q_2}{Q_1} = \langle e^{-(E_2-E_1)/kT} \rangle_1. \quad (9)$$

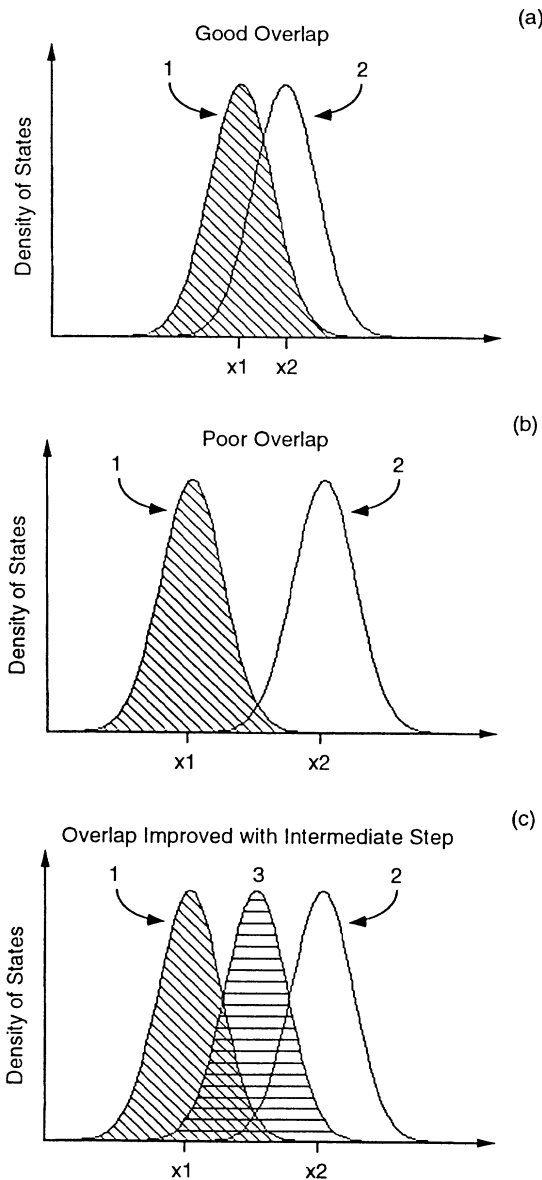


FIG. 2. Distributions of low-energy configurations for hypothetical one-dimensional ensembles: (a) Example of good overlap, (b) example of poor overlap, and (c) example of how overlap can be improved if an intermediate step is used.

Hence, a MC simulation can be used to sample this function over ensemble 1 and calculate the free energy difference ΔF . In one MC simulation the free energy difference can be calculated for every atom in the simulation cell. These are the $\Delta F(x)$ defined by Eq. (1) if the simulation is done on a surface simulation cell. If a simulation cell with no defects is used, $\Delta F(\text{bulk crystal})$ is calculated.

This technique works best if there is a large degree of overlap between the distributions of physical importance, that is, low-energy configurations for ensembles 1 and 2. Consider a pair of hypothetical ensembles that each have only one degree of freedom and a very simple distribution function (density of states). Suppose ensemble 1 has a distribution centered at x_1 and ensemble 2 has a distribution centered at x_2 . Figure 2(a) is an example of what a good degree of overlap between the two ensembles may look like. The thermodynamic average is performed for the low-energy configurations of ensemble 1 indicated by the cross hatching. Since the overlap is good, a large number of the low-energy configurations for ensemble 2 will also be sampled. Figure 2(b) shows an example of two ensembles with poor overlap. In this case very few of the low-energy configurations of ensemble 2 will be sampled and the statistics will not be good. For real ensembles with N atoms, there are $3N$ degrees of freedom and the distribution functions are not known. Thus, it is impossible to know *a priori* the degree of overlap of two different ensembles. In practice, it is necessary to perform the thermodynamic average for different length MC runs to determine the number of steps per atom required for a given degree of accuracy. The results of these calculations are exhibited in Fig. 3. It was determined for a standard deviation of 0.005 eV that the number of steps per atom must be $10^{3.2}$, $10^{3.7}$, and $10^{5.2}$ for the Ni(Cu), Pt(Au), and Ni(Pd) systems, respectively.

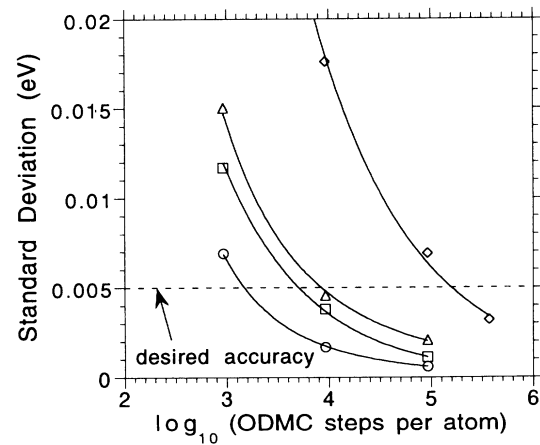


FIG. 3. Standard deviation (eV) vs number of steps per atom for the ODMC method. The circles, squares, diamonds, and triangles correspond to the alloy systems Ni(Cu), Pt(Au), Ni(Pd), and Ni(Pd) with an intermediate step, respectively. The level of accuracy that is used in this paper—0.005 eV—is shown by the dotted line.

Since the required number of steps per atom is very high for the Ni(Pd) system, the overlap was improved by using an intermediate step. Figure 2(c) illustrates how the overlap can be improved if an intermediate step is employed. The Helmholtz free energy difference is first calculated between ensembles 1 and 3 and then between ensembles 3 and 2. For Ni(Pd) the Helmholtz free energy calculations were performed using a *pseudo*-NiPd atom. This *pseudo*-NiPd atom was created by linearly averaging the EAM potential functions of Ni and Pd. The Helmholtz free energy difference was first calculated for the substitution of the pseudoatom for a Ni atom. In the second step the Helmholtz free energy difference was found for replacing the pseudoatom with a Pd atom. The total Helmholtz free energy difference is the sum of the differences for the two steps. Through the use of this intermediate step, the required number of steps per atom was reduced to $10^{3.9}$ for the Ni(Pd) system, as is also shown in Fig. 3.

C. Free-energy minimization method

The FEM method uses an approximate expression for the calculation of the Helmholtz free energy of a system. This approximate expression is what makes the technique much faster than MC or MD, but it also demands that it be thoroughly tested. With this methodology, the equilibrium configuration is found by minimizing this Helmholtz free energy with respect to the atomic positions, or the positions and compositions, using standard minimization techniques—for example, the conjugate gradient method. The derivation of the FEM method has been covered in detail elsewhere,^{13,14} so only a brief review is presented. The expression for the Helmholtz free energy is found as follows: First, the contribution to the Helmholtz free energy from the vibrational entropy (F_V) in the high-temperature classical limit is given by²⁵

$$F_V = kT \sum_{i=1}^N \sum_{\beta=1}^3 \ln \left[\frac{h\omega_{i\beta}}{2\pi kT} \right], \quad (10)$$

where the $\omega_{i\beta}$ are the vibrational frequencies of the atoms and h is Planck's constant. In the FEM technique, the vibrational frequencies are calculated by using an approximation to the quasiharmonic (QH) approximation, the local harmonic (LH) model. Like the QH approximation, the LH model utilizes the harmonic approximation keeping only the second-order terms but it also neglects the coupling of vibrations between atoms. By assuming that each atom is an independent oscillator, the required computation is reduced from the diagonalization of the full $3N \times 3N$ dynamical matrix to the evaluation of N local dynamical matrices that are only 3×3 , where N is the number of atoms in the ensemble.

The configurational entropy S_C , due to the different possible arrangements of atoms in a binary system, is calculated using a simple point approximation and the effective-atom concept and it is given by

$$S_C = -k \sum_{i=1}^N \{ C_A(i) \ln [C_A(i)] + C_B(i) \ln [C_B(i)] \}. \quad (11)$$

With the effective-atom concept we no longer deal with distinct types of atoms but with an "effective atom" on each atomic site. These effective atoms have concentrations C_A and C_B , where C_A is the time average probability that a site is occupied by an atom of type A , and $C_B (= 1 - C_A)$ is the probability that a site is occupied by an atom of type B . When the effective-atom concept is used, changes must also be made in the way the internal energy is calculated. The simple point approximation assumes that there is no spatial correlation in the occupation of atomic sites. This is only strictly correct for ideal solid solutions. In general S_C represents an approximation to the correct value of the configurational entropy; the experimental configurational entropy can be greater than or less than S_C .²⁶

To study solute-atom segregation, the transmutational ensemble is used. In this ensemble the total number of atoms and the relative chemical potential difference between the solvent and solute atoms are fixed, but the number of atoms of each species is allowed to vary. The proper thermodynamic potential for this ensemble is the grand potential:

$$\Omega = E + F_V - TS_C + \Delta\mu \sum_{i=1}^N C_A(i), \quad (12)$$

where $\Delta\mu$ is the chemical potential difference between the solute and solvent atoms.

In pure metals or alloys at the dilute limit of one component, there is no configurational entropy and the chemical potential difference term is a constant. Thus, to within a constant, the grand potential reduces to the Helmholtz free energy

$$F = E + F_V. \quad (13)$$

The equilibrium configuration is found by minimizing this potential with respect to the atomic positions. This is done by calculating the negative first derivative of Eq. (13) with respect to the positions and using the conjugate gradient method. The minimization is continued until the maximum atomic displacement in one step of any atom in the system is less than some tolerance, usually 10^{-3} or 10^{-4} nm.

To find the segregation free energy $F_B(x)$ from Eq. (1), $\Delta F(\text{bulk crystal})$ and $\Delta F(x)$ must be calculated. For $\Delta F(\text{bulk crystal})$ the Helmholtz free energy is calculated for a bulk crystal (no defects) both with and without a solute atom present. For $\Delta F(x)$ the Helmholtz free energy is calculated for a surface simulation cell both with and without a solute atom in the outermost surface plane. For the surface segregation profiles, $\Delta F(x)$ was also calculated for several subsurface planes by substituting the solute atom at appropriate sites.

Several computational difficulties were encountered in actually applying this methodology. The first difficulty stems from the fact that the FEM method is a minimization technique. Like all minimization techniques, the FEM method is sensitive to the initial conditions and care must be taken to ensure that the true equilibrium solution is found. The other problems that were encountered were numerical in nature. In the FEM method it is

necessary to calculate the third derivatives of the potential functions in order to find the forces on each atom. This raises problems with the way the EAM potentials used are usually treated; namely, the EAM potentials are stored in lookup tables. In the current work, a five-point Lagrange interpolation was used to obtain the higher-order derivatives. Another problem with the higher-order derivatives is inherent to the way these EAM potentials were determined. The embedding functions have points where the higher derivatives are discontinuous. Also, the real-space functions have discontinuous second and higher-order derivatives at the cutoff distance. The problem with the embedding functions was solved by fitting the functions to high-order polynomials plus a logarithmic term. The details of this fit are given in the Appendix. The problem with the discontinuities at the cutoff leads to problems in minimizing the energy in cases where interatomic separations are near the cutoff distance. This does not occur in the bulk but may occur at defects such as surfaces and grain boundaries. These computational difficulties, while making the FEM method somewhat more difficult to use, are not insurmountable.

III. RESULTS AND DISCUSSION

A. Effect of including local atomic relaxations and the vibrational entropy

The first effect on the simulation of surface segregation free energies that we examine is the effect of including local atomic relaxations. The simplest approach to simulating surface segregation free energies is to ignore local atomic relaxations and the vibrational entropy and just calculate the internal energy with the atoms located at their ideal lattice sites right up to the surface. A better approach is to include local atomic relaxations, so that the minimum energy configuration can be found. In

Table I the top value for each alloy is the segregation free energy calculated with no atomic relaxations. The bottom value is the segregation free energy calculated after allowing the atoms to relax to their equilibrium positions, employing a lattice statics simulation. As is shown by the values in bold, in over half of the 30 alloys, inclusion of local atomic relaxations strongly affects the calculated surface segregation free energies. For a few of the alloys, the effect of including local atomic relaxations changes the surface segregation free energy by 200% or more. In nearly all cases the change is in the direction of a weaker interaction between the solute and the free surface.

The second effect on the simulation of surface segregation free energies that we examine is the effect of including the vibrational entropy. To investigate this effect, we compare the results from the lattice statics simulations which include only local atomic relaxations to results from ODMC simulations which include both atomic relaxations and the vibrational entropy. In Table II the top value for each alloy is the segregation free energy calculated with lattice statics simulations. The bottom value is the segregation free energy calculated employing ODMC simulations. As is shown by the values in bold, the vibrational entropy strongly affects the calculated surface segregation free energies in a quarter of the 30 alloys. The alloys that are the most affected are the alloys with a small solvent (Cu or Ni) and a large solute (Ag, Au, Pd, or Pt). For these alloys, the effect of including the vibrational entropy changes the surface segregation free energy by 10% to 200%. Again, in most cases the change is in the direction of a weaker interaction between the solute and the free surface. The surface segregation free energy is changed by at least 0.01 eV for all but 13% of the alloys studied. Thus, for accurate calculations of surface segregation free energies, local atomic relaxations and the vibrational entropy must both be included in nearly all cases.

TABLE I. Effect of local atomic relaxations on (111) surface segregation energies. The top value for each alloy is the segregation energy calculated without atomic relaxations (atoms at ideal lattice positions). The bottom value is the segregation energy calculated with atomic relaxations from a lattice statics simulation. The bold values correspond to a difference of 0.05 eV or more. The values are in units of electron volts (eV).

Solute atom	Solvent atom					
	Cu	Ag	Au	Ni	Pd	Pt
Cu		-0.20	-0.24	0.12	-0.06	-0.03
		-0.09	-0.15	0.12	-0.02	0.00
Ag	0.32		0.07	0.45	0.29	0.39
	0.35		0.05	0.55	0.25	0.36
Au	0.46	-0.12		0.90	0.22	0.44
	0.35	-0.08		0.76	0.18	0.41
Ni	-0.08	-0.24	-0.28		-0.09	-0.08
	-0.07	-0.10	-0.16		0.00	-0.01
Pd	0.19	-0.30	-0.25	0.63		0.13
	0.12	-0.20	-0.20	0.50		0.15
Pt	-0.04	-0.53	-0.41	0.42	-0.18	
	-0.12	-0.34	-0.31	0.23	-0.15	

TABLE II. Effect of vibrational entropy on (111) surface segregation free energies. The top value for each alloy is the segregation energy calculated employing a lattice statics simulation that does not include the vibrational entropy contribution. The bottom value is the segregation free energy calculated at 1000 K employing an ODMC simulation that includes the vibrational entropy. The bold values correspond to a difference of 0.05 eV or more. The values are in units of electron volts (eV).

Solute atom	Solvent atom					
	Cu	Ag	Au	Ni	Pd	Pt
Cu		-0.09	-0.15	0.12	-0.02	0.00
Ag	0.35	-0.11	-0.14	0.10	-0.01	0.00
	0.33		0.05	0.55	0.25	0.36
Au	0.35	-0.08		0.05	0.26	0.37
	0.24	-0.11		0.76	0.18	0.41
Ni	-0.07	-0.10	-0.16		0.17	0.39
	-0.06	-0.11	-0.13		0.00	-0.01
Pd	0.12	-0.20	-0.20	0.50	0.01	-0.01
	0.04	-0.21	-0.18	0.36		0.15
Pt	-0.12	-0.34	-0.31	0.23	-0.15	0.15
	-0.19	-0.33	-0.28	0.09	-0.15	

B. Comparison of the FEM and ODMC methods

The results from the first part of this study indicate that in most cases it is necessary to use a simulation technique that includes both local atomic relaxations and the vibrational entropy for accurate calculations of surface segregation free energies. Unfortunately, most of the techniques that do this, such as the ODMC method, are very computer-resource intensive. Therefore, in the second part of this study we examine a new technique, the FEM method, which includes these effects, but makes some approximations enabling it to be more computer-resource efficient. Because of the approximate nature of the FEM method, we test its accuracy in calculating surface segregation free energies by making comparisons to results from the ODMC method.

The first comparison between the FEM and ODMC methods is of the segregation free energy at a (111) free surface for the set of 30 alloys. In Table III the top value for each alloy is the segregation free energy calculated with the FEM method. The bottom value is the segregation free energy calculated with the ODMC method. As shown by the bold entries, the two methodologies are in good agreement for 24 of the 30 alloys. The only alloys that do not show good agreement are those with a large solvent (Ag, Au, Pd, or Pt) and a small solute (Cu or Ni). For these alloys the segregation free energy difference is as large as 0.12 eV. For two of the alloys—Pd(Ni) and Pt(Ni)—the two simulation methodologies differ on which element will be enhanced at the surface.

Whenever possible, it is useful to compare simulation

TABLE III. Comparison of the FEM and ODMC methods for calculating the (111) surface segregation free energies at 1000 K. The top value for each alloy is the segregation free energy calculated from a FEM simulation. The bottom value is the segregation free energy calculated from an ODMC simulation. The bold values correspond to a difference of 0.02 eV or more. The values are in units of electron volts (eV).

Solute atom	Solvent atom					
	Cu	Ag	Au	Ni	Pd	Pt
Cu		-0.07	-0.02	0.10	-0.01	0.02
		-0.11	-0.14	0.10	-0.01	0.00
Ag	0.33		0.08	0.50	0.26	0.38
	0.33		0.08	0.50	0.26	0.37
Au	0.25	-0.11		0.59	0.17	0.40
	0.24	-0.11		0.58	0.16	0.39
Ni	-0.06		-0.06		-0.04	0.02
	-0.06	-0.11	-0.13		0.01	-0.01
Pd	0.04	-0.21	-0.18	0.36		0.16
	0.04	-0.21	-0.18	0.36		0.15
Pt	-0.19	-0.33	-0.28	0.09	-0.15	
	-0.19	-0.33	-0.28	0.09	-0.15	

TABLE IV. Component of selected fcc binary alloys that is enhanced due to segregation at free surfaces. A comparison is made between available experimental data and FEM and ODMC simulation results. The experimental data were taken from the compilations in Refs. 2, 7, and 10.

Alloy Solvent(Solute)	Enhanced surface component		
	Experiment	FEM result	ODMC result
Ag(Au)	Ag	Ag	Ag
Ag(Cu)	Ag	Ag	Ag
Ag(Pd)	Ag	Ag	Ag
Au(Ag)	Ag	Ag	Ag
Au(Cu)	Au	Au	Au
Au(Ni)	Au, Ni, or none	Au	Au
Au(Pd)	Au	Au	Au
Au(Pt)	Au	Au	Au
Cu(Ag)	Ag	Ag	Ag
Cu(Au)	Au	Au	Au
Cu(Ni)	Cu	Cu	Cu
Ni(Au)	Au	Au	Au
Ni(Cu)	Cu	Cu	Cu
Ni(Pd)	Pd	Pd	Pd
Pd(Ag)	Ag	Ag	Ag
Pd(Au)	Au	Au	Au
Pd(Ni)	Pd	Pd	Pd
Pt(Au)	Au	Au	Au
Pt(Cu)	Cu	Cu	None
Pt(Ni)	Pt, Ni, or none	Ni	Pt

results to experimental data. In Table IV the component that is enhanced due to segregation at free surfaces for several fcc binary alloys is shown. The experimental data have been taken from three compilations^{2,7,10} of published surface segregation data. These data were found with a variety of experimental techniques, conditions, and surface orientations. The simulation results are the same results presented in Table III for (111) surface segregation free energies. Negative segregation free energies indicate that the solvent will be enriched at the surface, and positive segregation free energies indicate that the surface will be enriched with solute. In all but three cases the experimental data and the two sets of simulation results are in perfect agreement. For the Au(Ni) alloy the experimental data are inconsistent, with either Au or Ni or no surface enrichment detected. Experiments²⁷ on Pt(Ni) show that the segregation profile is oscillatory and the enriched component is dependent on the surface plane. The experiments on (111) surfaces showed Pt enrichment on the outermost surface plane which is in agreement with the ODMC result. The experimental data are inconclusive for Pt(Cu). This might be expected since the simulation results predict that the amount of surface segregation for Pt(Cu) should be very low, making it difficult to measure experimentally. This comparison shows that both simulation methodologies are in excellent qualitative agreement with the available experimental data on surface segregation.

The second comparison between the FEM and ODMC methods is of segregation free energy profiles of (111) free surfaces for three alloys: Ni(Cu), Ni(Pd), and Pt(Au). These three alloys exhibit good agreement in the previous comparison for the outermost surface plane. The segre-

gation free energies of several (111) planes parallel to the surface are plotted as a function of the number of planes from the surface in Fig. 4. The $F_B(x)$ values calculated with the FEM method are always slightly greater than the values obtained from the ODMC method. The largest difference, which is for Ni(Pd), is about 0.02 eV. For all three alloys, the $F_B(x)$ value for the surface plane of atoms is large and positive, indicating that solute atoms have a strong tendency to segregate to the surface plane. The value of $F_B(x)$ for the second (111) plane is slightly negative for the Pt(Au) and Ni(Cu) alloys, while it is nearly equal to the bulk average for the Ni(Pd) system. This indicates that solute atoms are slightly repelled from the first subsurface plane in the Pt(Au) and Ni(Cu) systems. For the third plane and beyond, $F_B(x)$ approaches the bulk average value. This short-range oscillatory behavior in $F_B(x)$ may be the origin of some oscillatory segregation profiles that have been observed experimentally by Auger electron spectroscopy²⁷ or by the atom-probe field-ion microscopy technique.²⁸ This should not be confused with the long-range oscillatory profiles that are seen in ordering systems. Long-range oscillations are due to solute-atom interactions and cannot be present at the dilute limit that is being used in the current study. There is an expansion of less than one-half percent at the surface in the Ni(Cu) and Ni(Pd) alloys and a contraction of 4.6% in Pt(Au) in the direction normal to the surface. All three alloys also have an expansion of less than one-half percent at the center of the crystalline slab. This may be due to the finite thickness of the slab. The deviation of the bulk average values from zero is probably due to this expansion.

IV. CONCLUSIONS

We first investigated the importance of including local atomic relaxations and the vibrational entropy in the simulation of Helmholtz free energies of segregation for 30 face-centered-cubic dilute binary alloys at (111) free surfaces. With the simplest possible approach, an energy calculation with the atoms at their ideal lattice sites,

neglecting the local atomic relaxations, resulted in an overestimate of the surface segregation free energy for over half the alloys. If local atomic relaxations are included but the vibrational entropy is still neglected, as in a lattice statics simulation, the surface segregation free energy is still overestimated for nearly a quarter of the alloys. The effect of including the vibrational entropy was strongest for the alloys that have small solvent atoms and large solute atoms. We conclude that for an acceptable degree of accuracy in the calculation of surface segregation free energies, the simulation methodology must include local atomic relaxations in nearly all cases studied. The simulation methodology should also include the vibrational entropy in cases where the alloy has a small solvent atom and a large solute atom or in nearly all cases when a high degree of accuracy is desired.

Due to the conclusions of the first part of this study and the computer resources that are required by most simulation methodologies that include the vibrational entropy, in the second part of this study we investigated the accuracy and usefulness of a new technique, the FEM method. This methodology includes only an approximation for the vibrational entropy and therefore runs much faster than other techniques. Although it is an approximate technique, there have been only a few tests of its accuracy. By comparison with the more accurate ODMC method, we first investigated the accuracy of the FEM method in the calculation of surface segregation free energies for 30 face-centered-cubic dilute binary alloys. The two methodologies are in good agreement for all alloys except those that have large solvent atoms and small solute atoms. Both methodologies are in excellent qualitative agreement with available experimental data on surface segregation. A second comparison was made between the two methodologies by calculating surface segregation free energy profiles as a function of distance from the surface for three of the alloys. The segregation free energies calculated with the FEM method are always somewhat higher than the results from the ODMC method, but it is nearly a uniform shift in each case so that the profiles from each methodology have the same shape. From these comparisons we conclude that the FEM method is sufficiently accurate in calculating surface segregation free energies, except in cases where the alloy has a large solvent atom and a small solute atom.

Although the FEM method proved to be fairly accurate in these comparisons, there are several other factors that must be considered before applying it to other applications. These other factors can be divided into computational considerations and problems inherent in the methodology. The first computational consideration is that because the FEM method is a minimization technique, it is sensitive to the initial configuration and care must be taken that the final state is actually the true equilibrium configuration. There are also several numerical problems associated with calculating the higher-order (up to third) derivatives required by this methodology. While these computational considerations are not serious problems, they do make using this methodology somewhat more difficult.

There are more serious problems associated with the

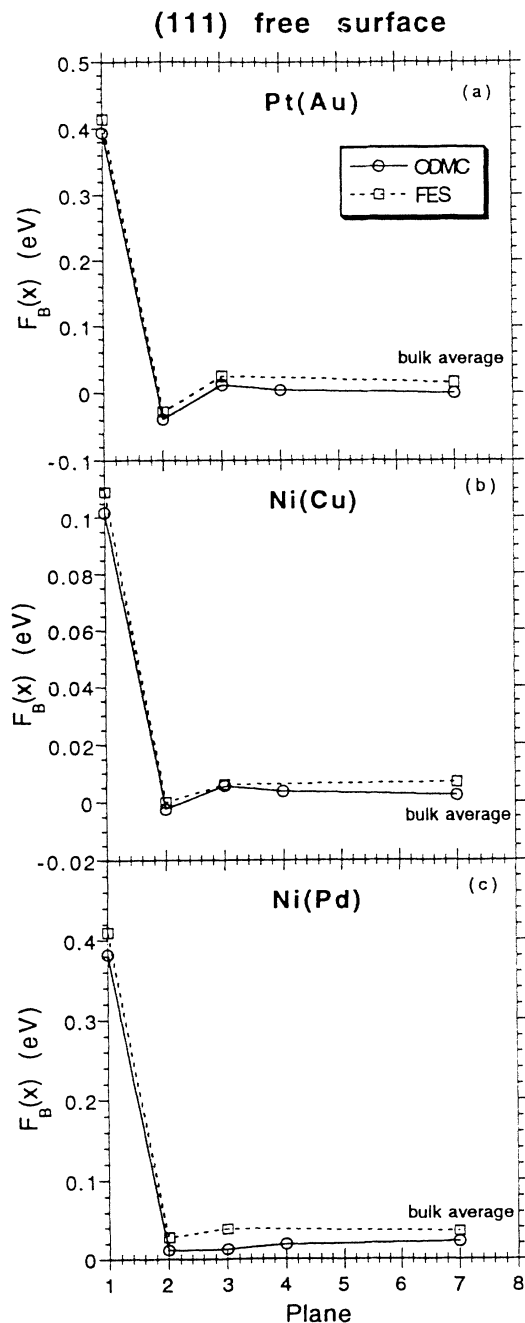


FIG. 4. Segregation free energy profiles for a (111) free surface: $F_B(x)$ vs plane. The values of $F_B(x)$ are averaged over (111) planes parallel to the surface and are plotted as a function of the number of planes from the surface. The circles and solid lines are for the ODMC simulations, while the squares and dotted lines are for the FEM simulations.

approximations that are made in the FEM method. In this study we only investigated the accuracy of the LH approximation for the vibrational frequencies in the vibrational entropy term as a function of different alloys. The calculations do not include any error associated with the point approximation for the configurational entropy or the effective-atom concept because all the simulations were performed at the dilute limit of one component in another. The point approximation does not accurately describe the true configurational entropy since it is only strictly correct for ideal solid solutions. The error associated with this approximation is expected to increase for compositions away from the dilute limit; this approximation can either underestimate or overestimate the experimental configurational entropy.²⁶ The effective-atom approach used to calculate the configurational entropy also affects the calculation of the internal energy. This introduces another source of error. It may be the case that these errors are even greater than the error associated with the LH approximation for the vibrational entropy. This is a question that requires further study.

As a final note, it is pointed out that recently²⁹ improvements to the LH approximation have been made. This modified local harmonic (MLH) model is said to improve the agreement with the quasiharmonic (QH) approximation. While it was shown to improve the agreement in the calculation of various bulk properties, there was no significant improvement in the calculation of vacancy formation free energies. This is because the corrections in the MLH model primarily affect only the vibrational frequencies of the bulk atoms. Thus, it appears that the MLH model would not improve the accuracy significantly for simulations involving geometries that deviate from the ideal bulk crystal, that is, simulations of vacancies, free surfaces, grain boundaries, etc. Also, the MLH model only improves the agreement with the QH model which is itself an approximation. In a recent study¹⁸ free energies were calculated for a bulk crystal, a vacancy, a (100) free surface, and a $\Sigma=5/(310)$ [001] symmetrical tilt boundary in Cu as a function of temperature using MC simulation techniques and the QH and LH approximations. It is found that the harmonic approximations substantially underestimate the temperature variation of the defect free energies as compared to the MC results. In a second study³⁰ free energies of a bulk crystal and (233) twin grain boundaries were calcu-

lated using the Stillinger-Weber Si potential and the QH, LH, and SM approximations at 1000 K. By comparison with MD thermodynamic integration results, it is found that the QH approximation produces accurate free energies whereas the free energies from the LH and SM approximations are unreliable.

From the results of the current study, the choice of alloy systems appears to be very important in determining the accuracy of this methodology. Alloys with large solvent atoms and small solute atoms may introduce large errors. Any alloy that deviates from the dilute limit would also be expected to increase the error of the calculations. From the other studies mentioned above, additional conclusions can be made. It appears that this methodology is best suited to calculating bulk properties. It also does a reasonably good job of calculating defect properties but only at relatively low temperatures. Despite the limitations mentioned, the FEM method is still very useful. Because of its computational efficiency, the FEM method is ideally suited for doing systematic studies of segregation thermodynamics that would presently be unfeasible with more computationally demanding techniques. It is important to know, however, how the results may be affected by the approximations that are being made.

ACKNOWLEDGMENTS

We would like to thank the United States Department of Energy for its support of this project through the following sources: The Computational Sciences Graduate Research program at Ames Laboratory, Ames, Iowa, for support of J.D.R; the Office of Basic Energy Sciences, Division of Materials Science, for support of S.M.F. through Contract No. DE-AC04-94AL85000; the Office of Basic Energy Sciences, Division of Materials Science, for support of D.N.S. through Contract No. DE-FG02-89ER45403, and the National Energy Research Supercomputer Center (NERSC) for computer time. Dr. B. Legrand, Dr. R. Najafabadi, Dr. D. J. Srolovitz, and Dr. D. Udler are thanked for useful comments on the manuscript.

APPENDIX

The numerical embedding functions that are part of the EAM potentials used in this work have discontinui-

TABLE V. The values of the coefficients used to fit the embedding functions of the EAM potentials used in this work. The a coefficient has units of eV nm³ and the b_i coefficients have units of eV. The coefficients are defined in Eq. (A1).

Coefficient	Ag	Au	Cu	Ni	Pd	Pt
a	0.153 618 5	0.126 875 8	0.096 906 5	0.159 198	0.059 377 07	0.111 393 22
b_0	-6.831 21	-9.185 55	-5.866 79	-6.689 31	-9.071 39	-11.889 8
b_1	-10.809 3	-9.595 03	-7.494 11	-10.383 6	-7.365 65	-10.984 42
b_2	2.849 57	-0.095 958 5	-1.367 89	-2.800 49	1.142 59	0.903 098
b_3	0.744 281	0.016 060 8	0.207 996	0.634 714	-0.463 842	0.254 642
b_4	-0.274 037	-0.169 241	-0.046 260 1	-0.205 456	0.091 483 2	-0.116 774
b_5	0.089 836 7	0.100 007	0.005 182 08	0.048 514 4	0.007 822 24	0.102 429
b_6	-0.018 630 2	-0.025 654 5	0.0	0.005 107 68	0.0	-0.029 683
b_7	0.001 695 47	0.002 549 38	0.0	0.0	0.0	0.003 178 6

ties in the derivatives. This is a result of the manner in which these functions were determined. The embedding function is obtained numerically by requiring that the energy versus volume for a uniform dilation fit a specified form. When the dilation or compression of the lattice caused a shell of neighbors to cross the cutoff distance for either the pair potential or the electron density, the embedding function has discontinuities in its higher-order derivatives. This is due to the fact that the pair potential and electron densities have discontinuous second and higher derivatives at the cutoff distance.

These discontinuities present a problem in the current work since they lead to discontinuities in the effective

force used to minimize the free energy. In addition, obtaining higher-order derivatives from the numerical tables was difficult. To address these issues, the embedding functions were fitted to the following form:

$$F(\rho) = a\rho \ln \left[\frac{\rho}{\rho_0} \right] + \sum_{i=0}^7 b_i \left[\frac{\rho}{\rho_0} - 1 \right]^i, \quad (\text{A1})$$

where $\rho_0 = 40 \text{ nm}^{-3}$. The fitting coefficients that were used for each element are given in Table V. The results obtained with these potentials are very similar to those obtained with the original potentials except that the numerical problems are reduced.

- ¹*Interfacial Segregation*, edited by W. C. Johnson and J. M. Blakely (American Society for Metals, Metals Park, OH, 1979).
- ²G. A. Somorjai, *Chemistry in Two Dimensions: Surfaces* (Cornell University Press, Ithaca, 1981).
- ³E. D. Hondros and M. P. Seah, in *Physical Metallurgy*, edited by R. W. Cahn and P. Haasen (North-Holland, Amsterdam, 1983), Pt. 1, Chap. 13, pp. 855–931.
- ⁴*Surface Segregation Phenomena*, edited by P. A. Dowben and A. Miller (CRC Press, Boca Raton, FL, 1990).
- ⁵G. Tréglia and B. Legrand, *Phys. Rev. B* **35**, 4338 (1987).
- ⁶G. Tréglia, B. Legrand, and P. Maugain, *Surf. Sci.* **225**, 319 (1990); B. Legrand and G. Tréglia, *ibid.* **236**, 398 (1990); *Phys. Rev. B* **41**, 4422 (1990); F. Ducastelle, B. Legrand, and G. Tréglia, *Prog. Theor. Phys. Supp.* **101**, 159 (1990).
- ⁷F. F. Abraham and C. R. Brundle, *J. Vac. Sci. Technol.* **18**, 506 (1981).
- ⁸F. F. Abraham, *Phys. Rev. Lett.* **46**, 546 (1981); F. F. Abraham, N.-H. Tsai, and G. M. Pound, *Scr. Metall.* **13**, 307 (1979).
- ⁹P. Wynblatt and R. C. Ku, *Surf. Sci.* **65**, 511 (1977).
- ¹⁰P. Wynblatt and R. C. Ku, in *Interfacial Segregation* (Ref. 1), pp. 115–136.
- ¹¹H. B. Huntington, G. Shirn, and E. Wajda, *Phys. Rev.* **99**, 1085 (1955).
- ¹²M. S. Daw and M. J. Baskes, *Phys. Rev. B* **29**, 6443 (1984); S. M. Foiles, M. I. Baskes, and M. S. Daw, *ibid.* **33**, 7983 (1986); M. S. Daw, *ibid.* **39**, 7441 (1989); M. S. Daw, S. M. Foiles, and M. I. Baskes, *Mater. Sci. Rep.* **9**, 251 (1993).
- ¹³R. LeSar, R. Najafabadi, and D. J. Srolovitz, *Phys. Rev. Lett.* **63**, 624 (1989).
- ¹⁴R. Najafabadi, H. Y. Wang, D. J. Srolovitz, and R. LeSar, *Acta Metall. Mater.* **39**, 3071 (1991).
- ¹⁵A. P. Sutton, *Philos. Trans. R. Soc. London Ser. A* **341**, 233 (1992).
- ¹⁶R. Najafabadi, D. J. Srolovitz, and R. LeSar, *J. Mater. Res.* **6**, 999 (1991); R. Najafabadi, H. Y. Wang, D. J. Srolovitz, and R. LeSar, in *High Temperature Ordered Intermetallic Alloys IV*, edited by L. Johnson, D. P. Pope, and J. O. Stieglar, MRS Symposia Proc. No. 213 (Materials Research Society, Pittsburgh, 1991), p. 51; H. Y. Wang, R. Najafabadi, D. J. Srolovitz, and R. LeSar, *Phys. Rev. B* **45**, 2028 (1992); *Philos. Mag. A* **65**, 625 (1992); *Metall. Trans. A* **23**, 3105 (1992); R. Najafabadi and D. J. Srolovitz, *Surf. Sci.* **286**, 104 (1993); H. Y. Wang, R. Najafabadi, D. J. Srolovitz, and R. LeSar, *Acta Metall. Mater.* **41**, 2533 (1993).
- ¹⁷R. Najafabadi, D. J. Srolovitz, and R. LeSar, *J. Mater. Res.* **5**, 2663 (1990).
- ¹⁸S. M. Foiles (unpublished).
- ¹⁹E. D. Hondros and M. P. Seah, *Scr. Metall.* **6**, 1007 (1972).
- ²⁰D. McLean, *Grain Boundaries in Metals* (Clarendon, Oxford, 1957).
- ²¹S. M. Foiles, *Phys. Rev. B* **32**, 7685 (1985); **40**, 11 502 (1989); in *Surface Segregation Phenomena* (Ref. 4), pp. 79–105.
- ²²B. Widom, *J. Chem. Phys.* **39**, 2808 (1963).
- ²³I. R. McDonald and K. Singer, *Discuss. Faraday Soc.* **43**, 40 (1967); *J. Chem. Phys.* **47**, 4766 (1967); **50**, 2308 (1969).
- ²⁴J. P. Valteau and G. M. Torrie, in *Modern Theoretical Chemistry*, edited by B. J. Berne (Plenum, New York, 1976), Vol. 5.
- ²⁵G. S. Rushbrooke, *Introduction to Statistical Mechanics* (Oxford University Press, London, 1949), Chap. 2, pp. 30–35; M. Born and K. Huang, *Dynamical Theory of Crystal Lattices* (Oxford University Press, London, 1954), Chap. 2, pp. 38–40; T. L. Hill, *Introduction to Statistical Thermodynamics* (Addison-Wesley, Reading, MA, 1960), Chap. 5, pp. 86–93.
- ²⁶C. P. Flynn, *Point Defects and Diffusion* (Clarendon, Oxford, 1972), pp. 28–34.
- ²⁷Y. Gauthier, Y. Joly, R. Baudoing, and J. Rundgren, *Phys. Rev. B* **31**, 6216 (1985); R. Baudoing, Y. Y. Gauthier, M. Lundberg, and J. Rundgren, *J. Phys. C* **19**, 2825 (1986); Y. Gauthier, R. Baudoing, M. Lundberg, and J. Rundgren, *Phys. Rev. B* **35**, 7867 (1987); Y. Gauthier, R. Baudoing, and J. Jupille, *ibid.* **40**, 1500 (1989).
- ²⁸T. T. Tsong, *Atom-Probe Field-Ion Microscopy* (Cambridge University Press, Cambridge, England, 1990), pp. 278–289; *Phys. Today* **46** (5), 24 (1993).
- ²⁹J. M. Rickman and D. J. Srolovitz, *Philos. Mag. A* **67**, 1081 (1993).
- ³⁰A. Hairie, F. Hairie, B. Lebouvier, G. Nouet, E. Paumier, N. Ralantson, and A. P. Sutton (unpublished).